Chinese Chemical Letters 33 (2022) 877–880

Contents lists available at ScienceDirect

Chinese Chemical Letters

journal homepage: www.elsevier.com/locate/cclet

Supramolecular self-assembling strategy for constructing cucurbit[6]uril derivative-based amorphous pure organic room-temperature phosphorescence complex featuring extra-high efficiency

Chunhui Li, Xiuqin Li, Qiaochun Wang*

Key Laboratory for Advanced Materials, Joint International Research Laboratory of Precision Chemistry and Molecular Engineering, Feringa Nobel Prize Scientist Joint Research Center, Frontiers Science Center for Materiobiology and Dynamic Chemistry, Institute of Fine Chemicals, School of Chemistry and Molecular Engineering, East China University of Science and Technology, Shanghai 200237, China

ARTICLE INFO

Article history:
Received 25 May 2021
Revised 4 August 2021
Accepted 5 August 2021
Available online 10 August 2021

Keywords:
Room temperature phosphorescence
Amorphous
Cucurbituril
Supramolecular self-assembling
Heavy-atom effect

ABSTRACT

The preparation of amorphous pure organic room-temperature phosphorescence materials with high efficiency is still a challenging task. Herein, we introduce a CB[6] derivative-based supramolecular self-assembling strategy. A water soluble and ellipsoidal deformed CB[6] derivative is used to self-assemble with 4-(4-bromophenyl)-1-methylpyridin-1-ium chloride, bromide and hexafluorophosphate in water. After freeze-drying, the obtained amorphous complexes exhibit brilliant green phosphorescence emission under ambient conditions, with phosphorescence efficiency up to 59%, 60% and 72%, respectively. This is the first report of amorphous non-polymeric pure organic room-temperature phosphorescence with such a high efficiency. In view of the dynamic self-assembling property, the complexes are responsive to water, which could enable information encryption.

Pure organic room-temperature phosphorescence (PORTP) materials, featuring large Stokes shifts, long triplet lifetime, diversified molecular design, lower cost and toxicity, have exhibited various potential practical applications, such as organic light-emitting diode (OLED), information encryption and anti-counterfeiting, and bio-imaging [1,2]. As is known to all, pure organic molecules usually suffer from inefficient RTP efficiency, owing to the inherently feeble spin-orbit coupling (SOC) and vulnerable triplet excitons [3]. Therefore, the key points to realize highly efficient RTP are to promote intersystem crossing (ISC) to populate triplet excitons, to minimize vibrational dissipation to restrict non-radiative relaxation, and to isolate triplet excitons from triplet oxygen to prevent quenching [4,5]. So far, the main strategies for efficient PORTP are focused on crystal engineering [6,7], halogen-bonds [8,9], co-polymerization or dope with rigid polymer [10–12], H-aggregation [13,14], host-guest complexation [15–18], and trace impurity-involved charge-separation [19,20]. There are only a few reports about PORTP materials with phosphorescence efficiency (Φ_p) exceeding 50%, however, these highly efficient PORTP materials are basically in high-quality crystal states [8,9,15,19,21,22], which require strict formation and maintenance conditions, thereby limiting their practical applications. Thus, it is crucial and challenging to construct highly efficient PORTP materials in amorphous state. As far as we know, the reports of amorphous highly efficient ($\Phi_p \geq 50\%$) PORTP materials are really rare. In 2013, Baldo dispersed phosphors into rigid poly(methyl methacrylate) (PMMA) to demonstrate an amorphous dopant with 50% RTP efficiency [23]. Recently, L proposed a synergistic strategy, involving cucurbit[6]uril (CB[6])-based host-guest complexation and copolymerization with acrylamide. The obtained amorphous polymer achieved a Φ_p up to 76% [24]. Nevertheless, to the best of our knowledge, there is still no report of non-polymeric amorphous highly efficient PORTP host-guest complex.

In this work, we put forward and demonstrated a supramolecular self-assembling strategy for constructing CB[6] derivative-based amorphous highly efficient PORTP host-guest complex. Non-phosphorescent 4-(4-bromophenyl)-1-methylpyridin-1-ium chloride (BMPCl) and hexafluorophosphate ($BMPPF_6$), and inefficiently phosphorescent bromide (BMPBr) were mixed in water with phenyl mono-functionalized cucurbit[6]uril (phCB[6]), respectively. After freeze-drying, the obtained amorphous host-guest complexes exhibited brilliant green phosphorescent emission, with Φ_p up

* Corresponding author.
E-mail address: qcwang@ecust.edu.cn (Q. Wang).

https://doi.org/10.1016/j.cclet.2021.08.011
1001-8417/

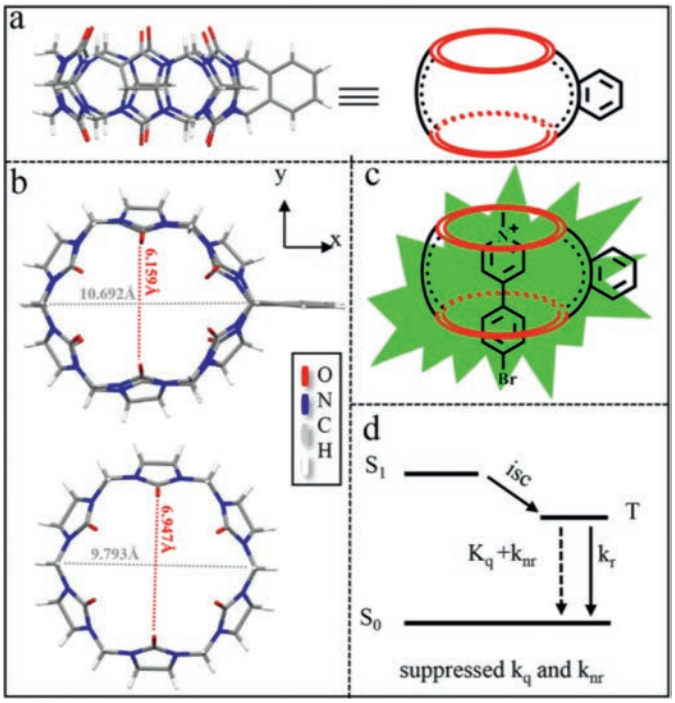

Scheme 1. (a) Single crystal structure and schematic illustration of phCB[6] (CCDC: 2084353); (b) Crystal structure view in *z*-axis and partial dimensional parameters for phCB[6] (top) and CB[6] (bottom, CCDC: 643862); (c) Schematic illustration of the complex showing RTP; (d) Simplified Jablonski diagram.

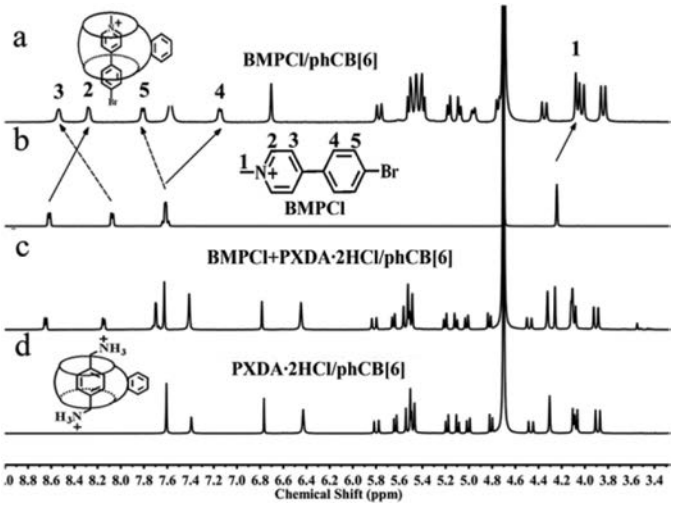

Fig. 1. ^{1}H NMR (D_2O, 400 MHz, 298K) of BMPCl/ phCB[6] (a), BMPCl (b), after adding 1 equiv. of PXDA·2HCl to BMPCl/phCB[6] (c), and PXDA·2HCl/phCB[6] (d).

to 59%, 60% and 72% for BMPCl/phCB[6], BMPBr/phCB[6] and $BMPPF_6$/phCB[6] under ambient conditions, respectively.

Herein, $BMPPF_6$, BMPCl, BMPBr and phCB[6] were synthesized by following previous reports [25,26]. The synthetic routes and characterization data are shown in Scheme S1 and Figs. S1–S4 (Supporting information). It was worth noting that we fortunately obtained the suitable single crystal of phCB[6] for X-ray diffraction (Scheme 1a and Table S1 in Supporting information). Although it was synthesized as early as 2011 by Issacs, the accurate X-ray structure was not determined. The phCB[6] is ellipsoidal deformed as compared to CB[6] (Scheme 1b) [27]. In addition, we were surprised to find that the water solubility of phCB[6] reaches up to 0.14 mol/L, in sharp contrast to CB[6] (1.8×10^{-5} mol/L) [28]. All these features imply that phCB[6] may overcome the disadvantage of poor binding affinity for CB[6] with phenyl guests (commonly as low as 10^2-10^3 L/mol) [29]. Once phosphor guests were encapsulated in the cavity of phCB[6] by self-assembling, the highly efficient PORTP host-guest complexes might be expected, owing to the strong restriction of vibrational dissipation and isolation of quenchers (Schemes 1c and d).

Benefiting from the good solubility of phCB[6], isothermal titration calorimetric (ITC) measurements were able to carried out in water to investigate the binding behaviors between guests and phCB[6]. Taking BMPCl as an example, The data were fitted to give a binding constant as 6.33×10^4 L/mol (Fig. S5a in Supporting information), indicating that BMPCl may form a stable host-guest complex with phCB[6]. Meanwhile, the ITC results also determines a stoichiometry of 1:1 for BMPCl and phCB[6], which is consistent with the result of UV–vis Job's plot (Fig. S5b in Supporting information). The results for BMPBr were similar with that of BMPCl, featuring a binding constant as 7.31×10^4 L/mol and a stoichiometry of 1:1 with phCB[6] (Figs. S5c and d in Supporting information).

To further clarify the binding mode of the host-guest complex, a series of measurements were also performed. The result of MALDI-TOF MS confirms the formation of the desired 1:1 complex BMPCl/phCB[6] (Fig. S6 in Supporting information). The 2D ^{1}H-^{1}H COSY NMR spectrum of the complex reveals the positional relationship of the aromatic protons of BMPCl in the complex according to the clear cross-peaks (Fig. S7 in Supporting information). The ^{1}H NMR measurements show that, as illustrated in Figs. 1a and b, the proton signals of BMPCl after complexation undergo significant upfield shifts by 0.16 ppm, 0.34 ppm and 0.48 ppm for methyl proton H_1 and aromatic protons H_2 and H_4, respectively. These changes in chemical shifts are in accord with those previous reports [15,30], thereby indicating a shielding effect owing to the deep encapsulation of BMPCl into the cavity of phCB[6]. The MS and ^{1}H NMR results for BMPBr/ phCB[6] were identical to that of BMPCl /phCB[6].

After uncovering the binding mode of the complexes, we firstly investigated their photophysical properties in aqueous solution (Fig. S8 in Supporting information). According to the binding constants obtained from ITC experiments, we set the concentration of BMPCl and BMPBr as 2.5×10^{-5} mol/L, while that of phCB[6] was 1.0×10^{-3} mol/L, so as to guarantee quantitative complexation at such a low concentration. The two complexes show a same emissive peak at 380 nm in the photoluminescent (PL) spectrum, when excited by the maximum excitation wavelength at 321 nm, which match well with the absorption spectra. Further time-resolved PL decay curves at 380 nm demonstrate the fluorescence characteristic, with nanosecond-scale lifetimes.

Before exploring the photophysical properties of the complexes in solid state, we firstly carried out powder X-ray diffraction (PXRD) to verify their amorphous states, featuring no obvious diffraction peaks (Fig. 2a). These three amorphous complexes BMPX/phCB[6] (X = Cl, Br, PF_6) all emitted brilliant green light when excited by 365 nm portable UV lamp under ambient conditions, implying a highly efficient PORTP (Figs. 2d and e, Fig. S14a in Supporting information). Taking BMPCl/phCB[6] as an example (Fig. 2d), there are two emissive peaks of 383 nm and 500 nm in the PL spectrum when excited by 334 nm. However, in delayed (0.1 ms) PL spectrum, only one emissive peak is centered at 503 nm. The subsequent time-resolved PL decay curves fitted a lifetime of 0.42 ns (Fig. S11a in Supporting information) for 383 nm and a lifetime of 9.2 ms for 506 nm (Fig. 2b), which demonstrate that they are fluorescence and phosphorescence, respectively. Moreover, the maintenance of the emission peak at 500 nm and the considerable enhancement of the lifetime of

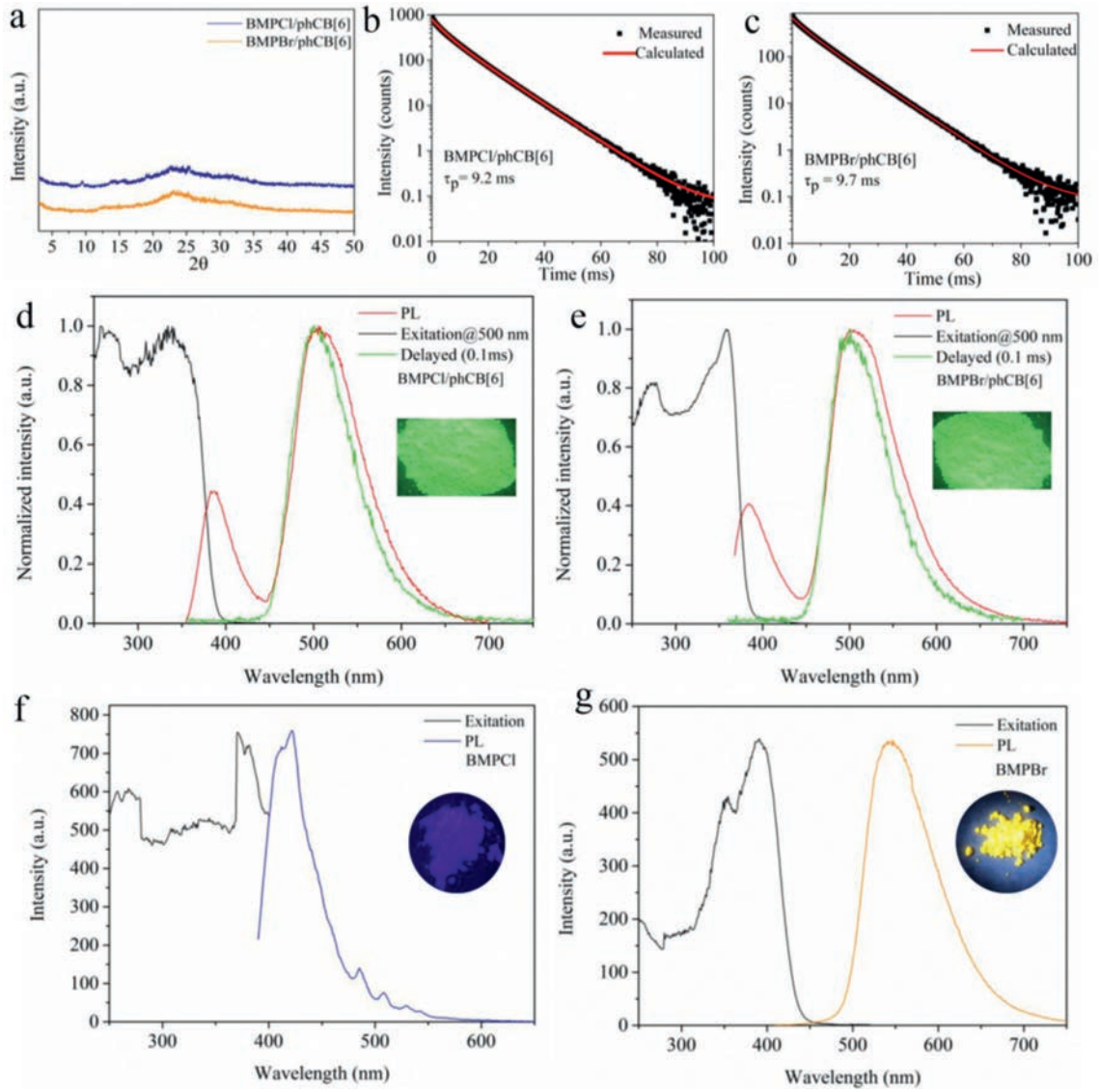

Fig. 2. (a) XRD patterns of the two complexes. Time-resolved PL decay curves of (b) BMPCl/phCB[6] and (c) BMPBr/phCB[6]; (d) Spectra of PL, excitation and phosphorescence for BMPCl/phCB[6] and (e) BMPBr/phCB[6] (inset: the photo of complexes under 365 nm UV lamp); Spectra of PL and exitation for (f) BMPCl and (g) BMPBr (inset: the photo of guests under 365 nm UV lamp).

Table 1
Photophysical data of BMPX/phCB[6] (X = Cl, Br, PF_6 and I) in solid state.

Substrates	λ_{ex} (nm)	λ_F (nm)	λ_P (nm)	τ_P (ms)	Φ_P (%)
BMPCl/phCB[6]	334	383	500	9.2	59
BMPBr/phCB[6]	358	384	501	9.7	60
$BMPPF_6$/phCB[6]	330	379	502	7.9	72
BMPI/phCB[6]	323	378	499	4.0	8.1

500 nm in 77 K further demonstrate the phosphorescence characteristic (Fig. S9 in Supporting information). As expected, the absolute Φ_p reaches up to 59% (Fig. S10a in Supporting information). The amorphous BMPBr/phCB[6] and $BMPPF_6$/phCB[6] own similar photophysical properties and high efficiency (Figs. S10b and S13 in Supporting information), as listed in Table 1. However, in the case of BMPI/phCB[6] (Fig. S13 and S14 in Supporting information), the Φ_p is only 8.1%, which could be attributed to the charge transfer from I^- to BMP^+ that greatly quench PL, according to the previous report [15]. By comparison, in the case of unbounding BMPCl (Fig. 2f), only slight bule fluorescence at 422 nm could be observed under excitation by 371 nm, with a lifetime of 0.47 ns (Fig. S11c in Supporting information). While for BMPBr (Fig. 2g), there is an emissive peak centered at 560 nm when excited by 391 nm. Combined with a lifetime of 0.15 ms (Fig. S11d in Supporting information), we could classify this emissive peak at 560 nm as phosphorescence, with an absolute Φ_p of 26.6%. The difference of photophysical properties between BMPCl and BMPBr may be attributed to the external heavy-atom effect from counter-ion Br^- [31]. Besides, it should be noted that there is no detectable optical signal for phCB[6] in the visible-light region (Fig. S12 in Supporting information), whether in aqueous solution or in solid state, indicating that the highly efficient PORTP originates form the BMPX (X = Cl, Br and PF_6) units in the cavity of phCB[6]. Meanwhile, the high performance of the complexes validate the phCB[6]-based supramolecular self-assembling strategy for highly efficient PORTP.

To verify the indispensable role of phCB[6] for the highly efficient PORTP, negative controlled experiments were conducted. Taking BMPCl/phCB[6] as an example, more than 1 equiv. of *p*-xylylenediamine hydrochloride (PXDA·2HCl) was added into the D_2O solution of the 1:1 complex. Proton signals of free BMPCl

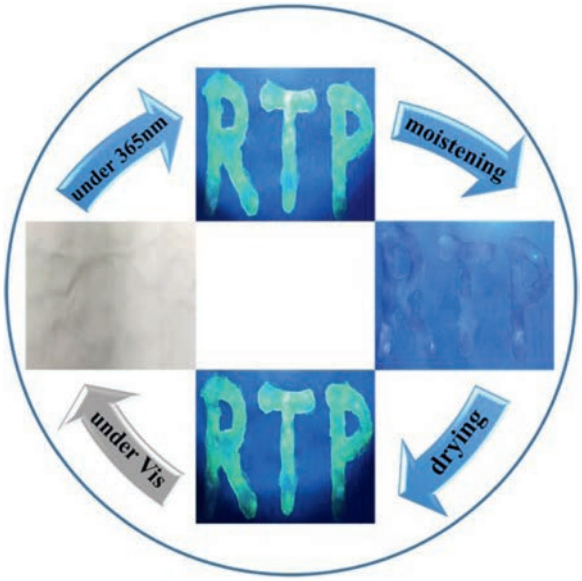

Fig. 3. Photographs of the word "RTP" written with the aqueous solution of BMPCl/phCB[6] under different lights and humidity conditions. The blue arrow represents a turn-on condition of UV lamp.

and another new set of PXDA·2HCl/phCB[6] complex appear in the ^{1}H NMR spectrum, (Figs. 1c and d) indicating that PXDA·2HCl could replace the occupation of BMPCl in the cavity of phCB[6] and simultaneously release BMPCl. The solid obtained after drying displayed blue luminescence, accompanied by the vanishment of the green emission. These facts prove that it is the host-guest interactions that are responsible for the boost of the RTP emission.

In view of the facts that water could quench the RTP of the complexes, we utilized the dynamic response properties and realized the information encryption. As illustrated in Fig. 3, the aqueous solution of BMPCl/phCB[6] was used as the encryption ink to draw a word "RTP" on a non-fluorescent paper. After drying, the word "RTP" was only visible under UV light and almost invisible under visible light. Besides, after moisten by water vapor for 30 s, the green emission of the word "RTP" disappeared under 365 nm UV light, while it reappeared by drying.

In summary, a phCB[6]-based supramolecular self-assembling strategy for highly efficient PORTP was proposed and demonstrated. Owing to the ellipsoidal deformation and fine water solubility of phCB[6], BMPCl, BMPBr and BMPPF$_6$ could self-assemble into the cavity of phCB[6] efficiently to minimize the vibrational dissipation and quenching of triplet excitons. Eventually, the first case of amorphous non-polymeric highly efficient PORTP host-guest complexes was realized successfully. Besides, owing to the dynamic self-assembling property in water, the aqueous solution of the complexes could be used as information encryption ink. We envision that the facilitation and the extra-high performance of this strategy will bring about inspiration for future RTP investigation.

Declaration of competing interest

The authors declare that they have no known competing financial interests or personal relationships that could have appeared to influence the work reported in this paper.

Acknowledgments

This work was financially supported by Shanghai Municipal Science and Technology Major Project (No. 2018SHZDZX03), National Natural Science Foundation of China (Nos. 21788102, 21572063), and the Fundamental Research Funds for the Central Universities.

Supplementary materials

Supplementary material associated with this article can be found, in the online version, at doi:10.1016/j.cclet.2021.08.011.

References

[1] M. Baroncini, G. Bergamini, P. Ceroni, Chem. Commun. 53 (2017) 2081–2093.
[2] S. Hirata, Adv. Opt. Mater. 5 (2017) 1700116.
[3] A. Forni, E. Lucenti, C. Botta, E. Cariati, J. Mater. Chem. C 6 (2018) 4603–4626.
[4] X. Ma, J. Wang, H. Tian, Acc. Chem. Res. 52 (2019) 738–748.
[5] T. Zhang, X. Ma, H. Wu, et al., Angew. Chem. Int. Ed. 59 (2020) 11206–11216.
[6] W. Yuan, X. Shen, H. Zhao, et al., J. Phys. Chem. C 114 (2010) 6090–6099.
[7] Z. Yuan, J. Wang, L. Chen, et al., CCS Chem. 2 (2020) 158–167.
[8] O. Bolton, K. Lee, H.J. Kim, K.Y. Lin, J. Kim, Nat. Chem. 3 (2011) 205–210.
[9] Z. Yang, C. Xu, W. Li, et al., Angew. Chem. Int. Ed. 59 (2020) 17451–17455.
[10] H. Wu, W. Chi, Z. Chen, et al., Adv. Funct. Mater. (2018) 1807243.
[11] Y. Su, S.Z.F. Phua, Y. Li, et al., Sci. Adv. 4 (2018) eaas9732.
[12] L. Ma, S. Sun, B. Ding, X. Ma, H. Tian, Adv. Funct. Mater. 31 (2021) 2010659.
[13] Z. An, C. Zheng, Y. Tao, et al., Nat. Mater. 14 (2015) 685–690.
[14] S. Cai, H. Shi, J. Li, et al., Adv. Mater. 29 (2017) 1701244.
[15] Z. Zhang, Y. Chen, Y. Liu, Angew. Chem. Int. Ed. 58 (2019) 6028–6032.
[16] J. Wang, Z. Huang, X. Ma, H. Tian, Angew. Chem. Int. Ed. 59 (2020) 9928–9933.
[17] J. Li, H. Zhang, Y. Zhang, W. Zhou, Y. Liu, Adv. Opt. Mater. 7 (2019) 1900589.
[18] W. Zhou, Y. Chen, Q. Yu, et al., Nat. Commun. 11 (2020) 4655.
[19] B. Ding, L. Ma, Z. Huang, X. Ma, H. Tian, Sci. Adv. 7 (2021) eabf9668.
[20] C. Chen, Z. Chi, K.C. Chong, et al., Nat. Mater. 20 (2021) 175–180.
[21] Y. Wen, H. Liu, S. Zhang, et al., J. Mater. Chem. C 7 (2019) 12502–12508.
[22] X. Ma, W. Zhang, Z. Liu, et al., Adv. Mater. 33 (2021) 2007476.
[23] S. Reineke, N. Seidler, S.R. Yost, et al., Appl. Phys. Lett. 103 (2013) 093302.
[24] Z. Zhang, W. Xu, W. Xu, et al., Angew. Chem. Int. Ed. 59 (2020) 18748–18754.
[25] Y. Zhang, T.Y. Zhou, K.D. Zhang, et al., Chem. Asian J. 9 (2014) 1530–1534.
[26] D. Lucas, T. Minami, G. Iannuzzi, et al., J. Am. Chem. Soc. 133 (2011) 17966–17976.
[27] D. Bardelang, K.A. Udachin, D.M. Leek, J.A. Ripmeester, CrystEngComm 9 (2007) 973–975.
[28] J.W. Le, S. Samal, N. Selvapalam, H.J. Kim, K. Kim, Acc. Chem. Res. 36 (2003) 621–630.
[29] J. Lagona, P. Mukhopadhyay, S. Chakrabarti, L. Isaacs, Angew. Chem. Int. Ed. 44 (2004) 4844–4870.
[30] Z. Zhang, Y. Liu, Chem. Sci. 10 (2019) 7773–7778.
[31] P. Xue, P. Wang, P. Chen, et al., Chem. Sci. 8 (2017) 6060–6065.